Adsorptive removal of copper(II) from aqueous solution onto the waste sweet lime peels (SLP): equilibrium, kinetics and thermodynamics studies

Dhanashree C. Panadare, Vikesh G. Lade, Virendra K. Rathod*

Chemical Engineering Department, Institute of Chemical Technology, Matunga, Mumbai 40019, India
Tel. +91 22 33612020; Fax: +91 22 33611020; email: vk.rathod@ictmumbai.edu.in

ABSTRACT

Heavy metal pollution has become one of the most serious environmental problems today. Keeping in view of the economic and pollution considerations; there is indeed need to develop process and practice for the waste management, for the disposal of industrial waste containing Cu(II) in a scientific manner. In the present study, sweet lime peels (SLP), an agricultural waste was utilized as an adsorbent for Cu(II) removal from aqueous solution. The biosorption mechanism and characteristics of SLP was studied by Fourier transform infrared. Kinetic studies based on pseudo-first-order and pseudo-second-order rate expressions have also been carried out. The pseudo-second-order kinetics was found to provide the best correlation with the experimental data. The effect of two parameters, namely, temperature (20, 30, 40, 50 and 60°C) and pH (2, 3, 4, 5, 6), were studied. The particle size effect in relation to biosorption capacity is also discussed. The experimental data were analysed using Langmuir, Freundlich, Redlich–Peterson, Temkin and Dubinin–Radushkevich isotherms. The Langmuir model was found to exhibit the best fit to experimental data. The maximum adsorption capacity was found to be 37.45 mg/g at 293 K. Thermodynamic parameters such as free energy ($\Delta G°$), enthalpy ($\Delta H°$) and entropy ($\Delta S°$) were also determined. Thermodynamic study showed that the biosorption was exothermic, spontaneous and favourable.

Keywords: Sweet lime peels (SLP); Kinetics; Adsorption isotherm; Adsorption thermodynamics

1. Introduction

Copper, one of the most widely used heavy metals; is mainly employed in electrical and electroplating industries [1]. Industrial waste streams including copper ore mining, metal cleaning, plating baths, paper and pulp, wood pulp production, fertilizer industry, etc. are the potential sources of copper [2,3]. Copper is essential to human life and is required for various biological processes; but like all heavy metals, it is potentially toxic for living organisms and ecological systems if present in larger amounts. Copper causes serious toxicological concerns such as widespread capillary damage; hepatic and renal damage; gastrointestinal irritation and corrosion; central nervous system irritation followed by depression; and deposits

*Corresponding author.

in brain, skin, liver, pancreas and myocardium [4–6]. Copper may be found as a contaminant in food, especially shellfish, liver, mushroom, nuts and chocolate [7]. Cu(II) is also harmful and toxic to fish life, aquatic flora and fauna even when its content is small in natural water resources [8]. According to World Health Organisation, International Standard of Drinking Water; the maximum permissible concentration of copper in drinking water is 1.0 ppm [9,10].

The wastewater from the process industries contains Cu(II) concentrations in the range of 100–120 mg/L. Current practices and methods for the removal of copper from contaminated water bodies are reverse osmosis, electro dialysis, ultrafiltration, ion-exchange, chemical precipitation, phytoremediation, membrane process, electrolysis and solvent extraction [11,12]. However, all these methods have their disadvantages such as incomplete metal removal, high chemical reagent requirement, energy requirements and inefficient and expensive, especially removing heavy metal concentrations less than 100 ppm. Therefore, there is need to find an efficient and low cost, easily available and eco-friendly adsorbent which is capable of removing copper ions from industrial wastewater [13,14].

Recently, researchers have reported that materials with biological origins, such as agricultural and animal waste, are effective and usable in the removal of heavy metals [8,15]. There is an increasing interest among the researchers to find low-cost bioadsorbents, viz. bark, tannin-rich materials, lignin, chitosan, dead biomass, algae, xanthate, zeolite, clay, fly ash, peat moss, bone beads, leaf mould, moss, modified wool and modified cotton, etc. [16]. The various researchers have carried out Cu(II) adsorption using agriculture waste such as apple wastes [17], banana peel [18], carrot residue [19], wheat shell [20], rubber leaves powder [21] and sour orange residue [22].

Citrus is subtropical and tropical crop, native to south-eastern Asia; with records of human cultivation extending back to at least 2,100 BC [23]. The worldwide production of citrus fruits has been increasing in about 140 citrus fruits producing countries [24]; and it is 106 million metric tons [25]. Citrus fruits are mainly used for dessert, juice and jam production [26]. The considerable amount of waste or by-products such as peels, seeds and pulps which represent 50% of the raw processed fruit is generated by citrus fruits and agro-food processing industry [27]. These by-products are considered as a valuable source of functional ingredients, namely, flavonoids, dietary fibres and essential oils. In the case of Korea, about 40,000 tons of citrus peel by-products out of 100,000 tons of citrus are being produced yearly in citrus juice processing

plants [28]. Accumulation of citrus fruit waste in the processing industries has resulted in two important problems which are land space occupation and pollution with phenolic compounds due to dumping of this waste. Since the sweet lime peels (SLP) are available free of cost from processing industries, only the drying and/or carbonisation is involved for the wastewater treatment. Hence, recycling of this solid waste for wastewater treatment would not only be economical but also will help to solve solid waste disposal problems.

Sweet Lime (*Citrus limettioides* Tanaka) is grown in India as Mitha nimbu mostly in Punjab and northern India and in the state of Tamil Nadu. In India, a number of large- and medium-scale sweet lime producing industries exist. It is also grown in Egypt, Palestine, Israel and neighbouring countries. Fruits are sweet or flat taste, medium sized, with few seeds. Peel is yellow to yellow-orange in colour, quite smooth, thin and adherent. Flesh is straw-yellow coloured. The disposal of fresh waste peels has become a major concern for many for the citrus processing industry [29]. The management of these wastes, which produce odour and soil pollution, represents a major problem for the citrus processing industry. There is growing interest in using large quantities of such kind of wastes available as low-cost, non-conventional alternative materials and can be used for the treatment of polluted water. This approach is an attractive and promising option with a double benefit for the environment.

The aim of this research is to investigate the possibility of using and transforming SLP waste to something valuable, namely, biosorbent. The present investigation envisages regarding the use of dried SLP available in large quantities for removal of Cu(II) ions from model waste water. The aim of the present investigation is to study the sorption kinetics, to establish the kinetic rate coefficients for sorption of Cu(II) by SLP, biosorption equilibrium employing different two-parameter isotherm models as well as thermodynamic studies.

2. Materials and methods

2.1. Chemicals

All chemicals used in the present work were of analytical purity. The stock solution of 1,000 ppm Cu(II) was prepared by using $CuSO_4$ $5H_2O$ and then diluted to appropriate concentrations for each test in double distilled deionised water. 1% phosphoric acid solution was prepared in deionised (DI) water for washing biosorbent. Acetate buffer of different capacities were used for pH value adjustment. The

analysis of Cu(II) was done by CHEMITO2700 spectrophotometer. PAN reagent used for spectrophotometric analysis was prepared by adding 300 ml of 1-(2-pyridrylazo)-2-naphthol (PAN) solution (4×10^{-3} mol/L), 50 ml of 1,4-dioxane 99.8% pure (HPLC grade) and 50 ml of sulphuric acid 0.2 mol/L. All chemicals were procured from Hi Media Laboratories, Mumbai, India.

2.2. Preparation of biosorbent from SLP

SLP collected from kitchen waste of nearby juice centre in Mumbai, were washed thoroughly with tap water and were dried in hot air oven for about 48 h. The dried SLP then were crushed in mixer and sieved so as to get adsorbent powder of different sizes; less than 0.355 mm, 0.355–0.71 mm and greater than 0.71 mm etc. The dried SLP adsorbent powder of uniform sizes were then soaked in 0.1 M phosphoric acid solution for 12 h for leaching of water-soluble colouring as well as aroma giving components. This was followed by leaching of remaining water-soluble components by water for 12 h. The biosorbent thus prepared by these methods was given several washings with tap water and finally with DI water. This is then air dried and used for further studies of adsorption.

Characterisation of biosorbent was done with FT-IR spectroscopy for determining the available functional groups on the surface of biosorbent. Perkin-Elmer's VERTEX80v FT-IR spectrophotometer was used in the range of 400–4,000 cm^{-1}. Sample preparation for FT-IR was done of KBr pressed pellet method. Used biosorbent particles were also analysed for the confirmation of utilised functional groups on surface area.

2.3. Detection of Cu(II) ions from model waste water

The detection of Cu(II) ions is done by spectrophotometric analysis with CHEMITO2700 spectrophotometer. Reagents required for analysis are PAN solution (4×10^{-3} mol/L), 1,4-dioxane 99.8% pure (HPLC grade) and sulphuric acid 0.2 mol/L. Stock solution of 1,000 ppm was prepared by dissolving copper (II) sulphate pentahydrate in DI water and standard solutions were prepared by proper dilution of stock solution in DI water. The standard curve for Cu(II) detection was prepared by serial dilution of standard solution in DI water as 100, 200, 300, … 1,000 ppm. 0.1 ml of every sample was added in 3 ml of PAN reagent, 0.5 ml of 1, 4-dioxane, 0.5 ml of sulphuric acid and DI water to make up the total volume of every sample as 5 ml. The samples were analysed at 560 nm spectrophotometrically.

2.4. Adsorption kinetics study

Kinetics is one of the important characteristics defining the efficiency of an adsorbent [30]. The study of sorption kinetics describes the adsorbate uptake rate and evidently this rate controls the residence time of adsorbate at the solid–liquid interface, hence the reactor dimensions are controlled by the system kinetics. It depicts the minimum time required for considerable adsorption to take place, uptake rate and controls the residual time of the whole adsorption process [31]. It gives insight into underlying adsorption mechanism involved in the process [32]. For designing of batch and continuous adsorption systems, the rate at which sorption takes place is an important factor to be considered.

In the present work, kinetic sorption studies were carried out using 100 ml of Cu(II) ion solutions of initial concentration 100 and 500 ppm. The metal ion solutions were measured into different labelled conical flasks containing 1.0 g of adsorbent. Both flasks with initial pH 6 were uniformly agitated in a temperature-controlled shaker at a speed of 200 rpm at 303 K. At predefined time intervals, the samples were withdrawn, filtered and analysed for Cu(II) uptake. The adsorption behaviour with time was checked and fitted into the kinetic model.

The equilibrium adsorption capacity was calculated using Eq. (1)

$$q_e = \frac{(C_o - C_e)V}{M} \tag{1}$$

The metal sorption capacity (q_t) of the biosorbent was calculated from the relationship Eq. (2)

$$q_t = \frac{C_o - C_t}{M} \tag{2}$$

Also, the Cu(II) percent removal (% RE) was calculated using the following Eq. (3)

$$\%RE = \frac{C_o - C_e}{C_o} \times 100 \tag{3}$$

2.5. Kinetic modelling

In order to clarify the biosorption kinetics of Cu(II) ions and the detail mechanism of adsorption rate for the adsorption onto SLP using two kinetic models [33], which are Lagergren pseudo-first-order and pseudo-second-order models, were applied to the experimental data.

The pseudo-first-order kinetic model considers the rate of occupation of the adsorption sites to be proportional to the number of unoccupied sites [34]. The linear form of the Lagergren pseudo-first-order rate equation [35–37] is given by Eq. (4)

$$\ln(q_e - q_t) = \ln q_e - k_1 t \tag{4}$$

Eq. (4) linearly correlates the values of $\ln(q_e - q_t)$ with t. The plot of $\ln(q_e - q_t)$ versus t will give a linear relationship from which k_1 and q_e can be determined from the slope and intercept of the graph, respectively.

The pseudo-second-order kinetic model assumes that the rate-limiting step may be biosorption involving valence forces through sharing or exchange of electrons between the biosorbent and adsorbate [38–41].

The linear form of the pseudo-second-order kinetics is given as:

$$\frac{t}{q_t} = \frac{1}{k_2 q_e^2} + \frac{t}{q_e} \tag{5}$$

If the pseudo-second-order kinetics is applicable to the experimental data, the plot of t/q_t versus t of Eq. (5) should give a linear relationship from which q_e and k_2 can be determined from the slope and intercept of the plot, respectively.

2.6. Batch adsorption experiments

The batch adsorption experiments were carried out by agitating 0.5 g of biosorbent with 50 ml of copper stock solution having different Cu(II) concentrations (100–1,000 mg/L) in a series of conical flask of 200 ml capacity at a temperature of $30 \pm 1°C$ at 200 rpm on a rotary orbital shaker. The flasks were agitated till 6 h to ensure the equilibrium. The effect of two parameters, namely, temperature (20, 30, 40, 50 and 60°C)

and pH (2, 3, 4, 5, 6), were studied. The experimental data were fitted in the different adsorption Isotherms. Using different buffering capacity of Acetate buffer; pH optimisation studies were carried out at fixed temperature of 30°C in temperature control orbital shaker incubator. For temperature optimisation study, initial pH was adjusted to be 5. To ensure that solutions are homogeneous and there is no air bubble in the sample, all solutions used were sonicated for about 20 min at 25 Hz in sonication bath before adsorption studies. After equilibrium, samples were withdrawn from the shaker and the adsorbent was separated from the solution by centrifugation at 5,000 rpm for 15 min. The biosorbent was separated and the filtrate was analysed by spectrophotometer for Cu(II) content. All experiments were replicated and the average results were used in data analysis.

2.7. Adsorption isotherm modelling

The graphical depiction of the equilibrium adsorption isotherm is done by plotting a solid phase concentration against liquid phase concentration [42]. There are many theories relating to adsorption equilibrium based on the mechanism of adsorption. Different adsorption isotherms like Langmuir [43], Freundlich, Redlich–Peterson (R–P) [44], Temkin [45] and Dubinin–Redushkevich (D–R) were studied and applied for pH and temperature studies. These isotherms as studied by other researchers [46–48] are represented in Table 1.

2.8. Desorption and reusability studies

As acidic solutions are reported to be the most efficient and well-known desorption agents in the literature [30,31], desorption of Cu(II) ions was checked with acidic solution of HCl, H_2SO_4, HNO_3 with 0.1 and 0.2 N concentration prepared in DI water. Used adsorbents were washed with deionised water

Table 1
Different adsorption isotherms models with their equations

Isotherm	Equation	Equation in linear form	Graph drawn
Langmuir	$q_e = \frac{q_{max} K_L C_e}{(K_L C_e + 1)}$	$\frac{C_e}{q_e} = \left[\frac{1}{K_L q_{max}}\right] + \left[\frac{1}{q_{max}}\right] C_e$	$\frac{C_e}{q_e}$ vs C_e
Freundlich	$q_e = K_F C_e^{\frac{1}{n}}$	$\ln q_e = \ln K_F + \frac{1}{n} \ln C_e$	$\ln q_e$ vs $\ln C_e$
Redlich–Peterson	$\frac{c_e}{q_e} = \frac{1}{K_{R-P}} + \left(\frac{\alpha_R}{KR-P}\right) C_e^{\beta}$	$\ln\left(\frac{C_e}{q_e}\right) = K_{R-P} + \beta \ln C_e$	$\ln\left(\frac{C_e}{q_e}\right.$ vs $\left. \ln C_e\right)$
Temkin	$q_e = \left(\frac{RT}{b}\right) \ln K_T + \left(\frac{RT}{b}\right) \ln C_e$	$q_e = A \ln K_T + A \ln C_e$ where, $A = \frac{RT}{b}$	q_e vs $\ln C_e$
Dubinin–Redushkevich	$\ln q_e = \ln q_{max} - B\varepsilon^2$	$\ln q_e = \ln q_{max} - B\varepsilon^2$ where, $\varepsilon = RT \ln\left[1 + \frac{1}{C_e}\right]$ $E = 1/\sqrt{2B}$	$\ln q_e$ vs ε^2

and filtered. About 1 g adsorbent was taken in a 250 ml flask and added with 50 ml desorption solution. Samples of 200 μl were withdrawn after regular time intervals and analysed for Cu(II) ions. The reusability of biosorbent was checked for five cycles of adsorption–desorption.

Adsorption was carried out in 250 ml conical flask with 100 ml of 500 ppm copper ions solution. Used adsorbents were then filtered and washed with DI water and used for desorption. 0.1 N HCl was used for desorption. After desorption, the biosorbent was washed with DI water and again used for adsorption.

3. Results and discussion

3.1. Fourier transforms infrared (FT-IR) analysis

In order to determine the functional groups responsible for metal uptake, the FT-IR spectra of unloaded and Cu(II)-loaded *SPL* in the range of 400–4,000 cm^{-1} were taken and compared with each other to obtain the information on the nature of the possible adsorbent–metal ion interactions and presented in Fig. 1. Unloaded bioadsorbent SPL and SPL treated with 100 mg/L solutions of Cu(II), respectively, were analysed. The chemical functional group tends to absorb infrared radiation in a specific wavelength range as infrared light interacted with the unloaded SLP, it caused stretching, contraction and bending of its chemical bonds and it is represented in Table 2. The spectra indicate the presence of different functional groups which are responsible for metal sorption process. The very broad peak around

3,428 cm^{-1} indicates the existence of free and intermolecular bonded OH groups. The peak that corresponds to this functional group was altered after Cu(II) adsorption indicating their involvement in Cu(II) binding. The inclusion of hydroxyl groups on the metal binding was also observed by Prasad and Freitas [49] and Aydin et al. [50]. The oxygen on each hydroxyl group acts as a strong Lewis base because of the presence of its vacant double electrons, and this hydroxyl group undergoes a complex coordination with metal Cu(II), which is electron deficient [51]. The peaks observed at 2,972 cm^{-1} can be assigned to aliphatic C–H groups, –CH$_2$ vibrations (2,922 cm^{-1}), methoxy group band (2,851 cm^{-1}), Carboxyl stretching groups(1,739 cm^{-1}), –C–C stretch (1,560 cm^{-1}), C–C vibration (1,465 cm^{-1}), esters (1,299 cm^{-1}), ethers (1,076 cm^{-1}), thioesters (880 cm^{-1}) and alkyne (669 cm^{-1}). The absorbance peaks in the Cu(II)-loaded sample are lower than those in the unloaded sample of the bioadsorbent. This indicates that the bond stretching occurs to lesser degree due to the presence of Cu(II). The disappearance of the 1,076 cm^{-1} band suggests that the C–O stretching of ether group is the main cause for Cu(II) adsorption onto the SLP. The carboxylic group was found to be the major metal-binding site [52].

3.2. Adsorption kinetics

Two kinetic models, namely; pseudo-first-order [53] and pseudo-second-order, [38] are selected in this study for describing the adsorption process.
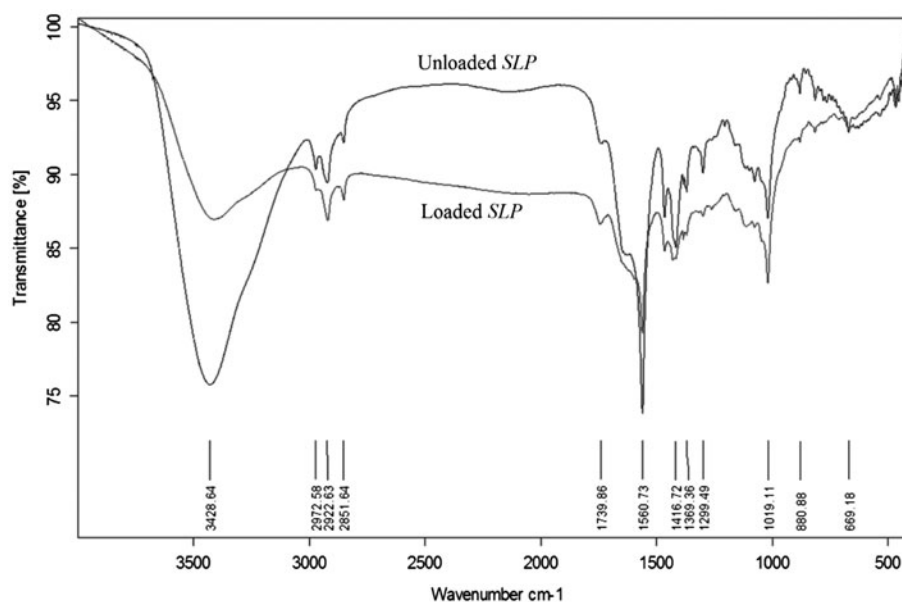
Fig. 1. FT-IR spectra of unloaded SLP and Cu(II)-loaded *SLP*.

Table 2
Major functional groups in SLP and Cu(II) adsorbed SLP biosorbent

Functional group	Band position, wavenumber (cm^{-1})	
	Unadsorbed SLP biosorbent	Cu(II) adsorbed SLP biosorbent
O–H stretch (cellulose)	3428.65	3411.19
C–H Stretch (aliphatic)	2972.58	2969.51
CH$_2$ vibration	2922.64	2920.88
Methoxy group	2851.63	2850.91
Carboxyl stretching groups	1739.85	1743.46
C–C stretch (aromatics structure)	1560.77	1550.95
C–C vibration	1465.26	1464.93
C–O stretch	1299.51	1299.12
C–O stretch of metal–carboxylate complex (COO–Cu)	1076.27	–
–OH bend (carboxylic acids)	1019.07	1018.93
Thioesters	880.89	465.62
Alkyne	669.37	669.28

3.2.1. The effect of Cu(II) initial concentration and contact time

The adsorption kinetic study was undertaken in a batch reactor (250 ml) and performed at 30 °C. The required amounts of the SLP adsorbent were weighed accurately and were placed in cylindrical glass reactor containing copper solution. At different time intervals, the samples were collected and were then analysed for Cu(II) concentration.

Fig. 2 shows the influence of contact time on the adsorption of Cu(II) onto SLP investigated at two initial concentrations of Cu(II), namely, 100 and 500 mg/L. It can be seen that, with an increase in the initial Cu(II) concentration, from 100 to 500 mg/L; the equilibrium adsorption capacity of SLP increased from 8.08 to 28.88 mg/g and the percentage removal decreased from 87.79 to 57.76% within 30 min. The higher initial concentration of Cu(II) ions will enhance the adsorption process as it provides more driving force to overcome all mass transfer resistances of Cu(II) ions between the aqueous and solid phase [54], but its rate gradually decreases with passage of time reaching a maximum. Similar results were obtained by Demirbas et al. [31] and Tong et al. [14]. Steepness decreases drastically from 30 to 120 min and then gradually becomes constant. The initial faster rate may be due to the availability of the uncovered surface area of the adsorbent initially, since adsorption kinetics depends on the surface area of the adsorbent. In addition, the variation in the amount of Cu(II) ion removed the adsorbent could be related to the nature and concentration of the surface groups (active sites) responsible for the interaction with Cu(II).

3.2.2. Kinetic model fitting

The kinetic data obtained from Cu(II) adsorption experiments were analysed using the pseudo-first-order kinetic model according to Eq. (4) and is illustrated in Fig. 3. From the plot, the pseudo-first-order rate constant, k_1, and the sorption capacity, q_e, were computed from the slope and intercept of the plot and shown in Table 3. The value of the correlation coefficient of Cu(II) was found to be 0.82, which is very small as compared to standard correlation coefficient which is equal to 1. There is about 75.6% difference in
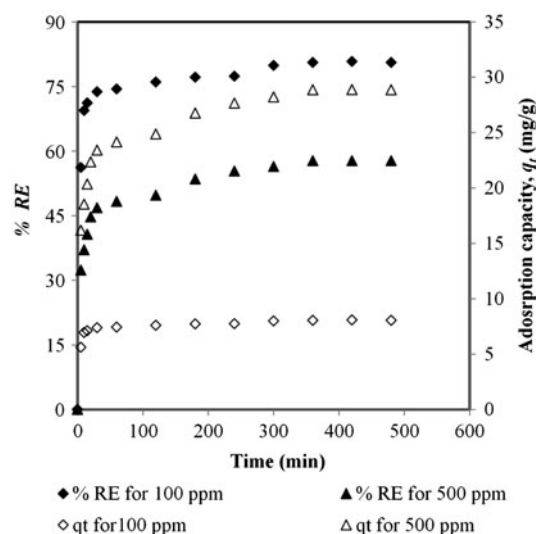
Fig. 2. Effect of contact time for the adsorption of Cu(II) ions at different initial concentrations (initial pH of solution = 6, adsorbent dosage = 1 g, temperature = 30 °C, agitation rate = 200 rpm).
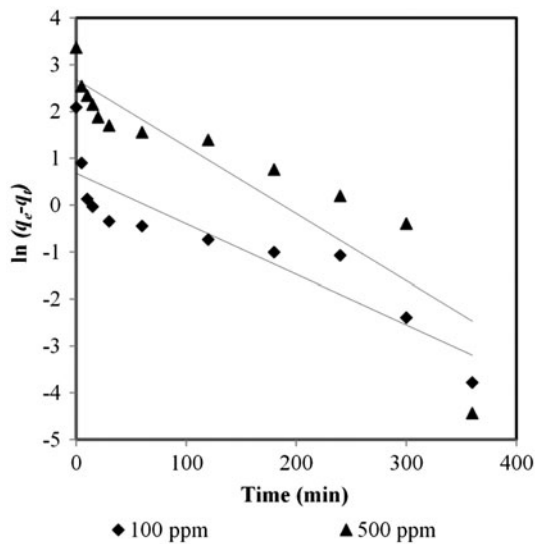
Fig. 3. The pseudo-first-order kinetic model fitting for the adsorption of Cu(II) onto SLP at various initial copper concentrations.

Table 3
The pseudo-first-order and pseudo-second-order kinetic parameters for Cu(II) at different initial concentrations

Kinetic model	C_0 (mg/L)	
	100	500
q_e experimental (mg/g)	8.08	28.88
Pseudo-first-order		
q_e calculated (mg/g)	1.97	14.64
k_1 (min^{-1})	0.011	0.014
R^2	0.82	0.82
Pseudo-second-order		
q_e calculated (mg/g)	8.10	29.32
k_2 (g/mg min)	0.028	0.0035
$h = k_2 q_e^2$ (mg/g min)	1.81	3.03
R^2	0.99	0.99

the calculated adsorption value ($q_{e,cal} = 1.97$ mg/g) and experimental value ($q_{e,exp} = 8.08$ mg/g) for the initial concentration of 100 ppm. From these results, it can be said that the adsorption of Cu(II) onto the SLP is not a first-order reaction which can be explained by the behaviour of parameter k_1. Higher the value of parameter k_1, which is time scaling factor, shorter is the time required for the system to reach the equilibrium [55]. Plazinski et al. [55] reviewed the theoretical description and fundamental consideration on the pseudo-first-order and pseudo-second-order models. The satisfactory predictability of first-order model can be given only if the system is not very close to equilibrium which is not fulfilled by our experimental data as indicated in Fig. 3. The applicability of the pseudo-first-order equation depends on the range time at which the data recorded [51].

Fig. 4 depicts the plot of t/q vs. contact time for the pseudo-second-order equation for the sorption of Cu(II) ions. From the plot, the values of the pseudo-second-order rate constant k_2, the initial adsorption rate h and the sorption capacity q_e computed from the slope and intercept are presented in Table 3. The experimental data showed a good compliance with the pseudo-second-order equation and the correlation coefficients for the linear plots were about 0.99 for both initial concentration conditions. The rate constant (k_2) value of Cu(II) increased with increasing concentration. It is observed from the graph that biosorption strictly followed the pseudo-second-order kinetics and not at all the pseudo-first-order. The maximum adsorption capacity calculated from graph

Fig. 4. The pseudo-second-order linear equation obtained by the linear method for the adsorption of Cu(II) onto SLP at various initial copper concentrations.

resembles the maximum adsorption capacity observed during the experimentation. The highest second-order rate constant (k_2) for Cu(II) was found to be 0.028 g/mg min at 30℃. These results indicate that $q_{e,cal}$ are close to the $q_{e,exp}$. The experimental data for the adsorption kinetics of Cu(II) on SLP fit the pseudo-second-order kinetic model. The pseudo-second-order model was based on the assumption that biosorption followed a second-order mechanism, which meant that the rate of occupation of adsorption sites was proportional to the squares of number of unoccupied sites [56].

3.3. Batch adsorption studies and its modelling

The influence of several operational parameters, viz. temperature, initial pH, and time on biosorption of Cu(II) ions by SLP is investigated. The experimental data points were fitted to the Langmuir, Freundlich, R–P, Temkin and D–R isotherm equations. The linear equations of the four isotherm models are listed in Table 1. The constant parameters of the isotherm equations were evaluated.

3.3.1. Effect of particle size

As adsorption capacity mainly depends upon the total available surface area for adsorption; which in turn mainly depends on the amount and size of adsorbent. Three different sizes of adsorbents were selected as, less than 0.355 mm, 0.355–0.71 mm and greater than 0.71 mm, etc. The initial concentration of 600 ppm was taken to check the maximum adsorption capacity with initial pH 5 at 30℃ for 7 h. The unadsorbed Cu(II) ions concentration was checked spectrophotometrically. Preliminary adsorption studies of Cu(II) ions onto the SLP indicated that sorption capacity is dependent on its particle size.

The sample with particle size less than 0.355 mm gave the maximum adsorption capacity (31.94 mg/g) and this is attributed to the larger surface area of the adsorbent. The adsorption capacity for the biosorbent size 0.355–0.71 mm was found to be 29.85 mg/g. Decrease in the size of biosorbent increases the adsorp-tion capacity by 7%, while increase in size to 0.71 mm decreases the adsorption capacity (25.42 mg/g) by 15%. Diffusional resistance to mass transfer in the case of adsorbent with larger particle sizes is higher and most of the internal surface of these particles may not be utilised for adsorption. Consequently, the amount of metal ions adsorbed is less in such cases. Since the extent of adsorption is considerably higher in the case of SLP samples of 0.355 mm particle sizes, it was decided to limit the discussions of the adsorption experiments to that with SLP of 0.355 mm particle size.

3.3.2. Effect of pH on the adsorption capacity

pH is an important parameter affecting the adsorption of metal ions from aqueous solution [57]. This is partly because hydrogen ions themselves are strongly competing with adsorbate [58]. The results are expressed as the amount of Cu(II) ions adsorbed on SLP biosorbent at any time (q, mg/g), adsorbed Cu(II) ions per gram of SLP at equilibrium (q_e, mg/g) and concentration of Cu(II) ions that remain in solution at the equilibrium (C_e, mg/L). The constant parameters of Langmuir, Freundlich, R–P, Temkin and D–R isotherm equations are calculated and represented in Table 4.

The uptake and percentage removal of Cu(II) from the aqueous solution are strongly affected by the pH of the solution. The influence of the pH on adsorption

Table 4
Constants and regression coefficients for different adsorption isotherms at different pH

Isotherm	Parameters	pH 2	pH 3	pH 4	pH 5	pH 6
Langmuir	q_{max} (mg/g)	21.14	21.55	24.27	24.33	21.79
	K_L (L/mg)	0.05	0.17	0.30	0.79	0.78
	R_L	0.0358	0.0116	0.0065	0.00253	0.00256
	R^2	0.97	1.00	1.00	1.00	1.00
Freundlich	n	1.71	2.64	2.20	4.40	4.82
	K_F (L/g)	1.61	4.53	4.16	10.33	9.83
	R^2	0.90	0.91	0.76	0.91	0.92
Redlich–Peterson	β	0.41	0.62	0.54	0.78	0.79
	K_{R-P} (L/g)	0.47	1.51	1.42	2.34	2.29
	R^2	0.82	0.97	0.82	0.99	0.99
Temkin	A (L/mg)	2.25	5.88	22.72	29329.30	59016.80
	$K = RT/b$	0.06	0.04	0.05	0.02	0.02
	R^2	0.90	0.91	0.76	0.92	0.92
Dubinin–Radushkevich	q_{max} (mg/g)	17.86	19.83	26.58	23.01	20.80
	B	0.0029	0.0012	0.002	0.0003	0.0003
	E (kJ/mol)	0.43	0.67	0.52	1.33	1.33
	R^2	0.98	0.98	0.96	0.99	0.99

of Cu(II) onto SLP adsorbent related to two factors. First one is the charge of surface functional groups (i.e. hydroxo, carboxo) onto the SLP biosorbent cell wall and the second one is metal ion chemistry in solution [59]. The pH of the aqueous medium affects the solubility of metal ions. The concentration of the counter ions on the functional groups of the SLP bioadsorbent cell walls is also affected by pH.

The capacity of Cu(II) removal at the equilibrium increases with the initial *pH* from 2 to 5, beyond that capacity decreases at pH 6 as shown in Table 4. The maximum Cu(II) adsorption was found to occur at pH around 4–5. The optimum pH for the Cu(II) adsorption in our study was found to be 4–5; which is also found by different investigators for the different biosorbents (Table 5).

At lower initial pH, in the solution, Cu(II) exists as different anion species and the surface of the adsorbent would also be surrounded by H_3O^+ ions which decrease the Cu(II) interaction with binding sites of the adsorbent hindrance effect and repulsive force. As the pH increased, the overall surface on the sorbent became negative and sorption increased. On the other hand, at higher pH, copper hydroxides are formed thereby both species are adsorbed at the surface of adsorbent [66].

At different pH, the experimental data points were fitted in Langmuir isotherm (Fig. 5) and isotherm constants, correlation coefficient are presented in Table 4.

The maximum Cu(II) adsorption capacity of SLP is equal to 24.33 mg/g at pH 5. The results suggest that the pH has very limited effects on the adsorption capacity of Cu(II) onto the SLP. In general, the amount of Cu(II) adsorbed increased as the pH increased, and sharply reached the maximum adsorbed concentration equal to 24.33 mg/g at pH 5 from 21.14 mg/g at pH 2 and then again decreased to 21.79 mg/g at pH 6. The low removal efficiency observed at low pH can be attributed to the competition between H^+ and Cu^{2+} ion on the surface sites [3]. Indeed, at pH < 4, the Cu(II) removal was relatively less, whereas the removal increased in the pH range from 4 to 5.

The equilibrium parameter used to predict if an adsorption system is favourable or unfavourable which is essentially expressed in terms of Langmuir model constant is termed as separation factor (R_L) [21,67] and expressed by Eq. (6)

$$R_L = \frac{1}{(1 + C_o K_L)} \tag{6}$$

For all the experimental pH conditions, the values of R_L lie between 0 and 1 (see Table 4) for the initial copper concentration range from 100 to 1,000 mg/L, signifying favourable adsorption of copper onto SLP.

The adsorption of Cu(II) onto the SLP adsorbent was also analysed by the Freundlich isotherm

Table 5
Different biosorbents with their maximum adsorption capacity and optimum pH

Biosorbent	Adsorption capacity (mg Cu(II)/g adsorbent)	Optimum pH	Reference
Apple wastes	10.8	5.5–7	Lee and Yang [17]
Banana peel	4.75	6–8	Annadural et al. [18]
Capsicum annuum Seeds	8.2	5	Özcan et al. [58]
Carrot residue	32.7	3–5	Nasernejad et al. [19]
Cassava peel (*Manihot esculenta*)	41.77	4.5	Kosasih et al. [51]
Collagen–tannin resin	16.52	5	Sun et al. [60]
Cotton boll	11.4	6	Ozsoy and Kumbur [54]
Dehydrated wheat bran	51.5	5	Özer et al. [61]
Dried sunflower leaves	89.37	5–6	Benaïssa and Elouchdi [35]
Grapeseed activated carbon	32.15	5	Özçimen and Ersoy-Meriçboyu [62]
Hazelnut shell activated carbon	15.33	5.8	Demirbas et al. [31]
Orange peel xanthate	77.6	5–5.5	Liang et al. [63]
Peanut hull	21.25	5.5	Zhu et al. [36]
Pine cone powder	5.76	3–5	Ofomaja et al. [64]
Pineapple leaf powder	9.28	5	Weng and Wu [65]
Rubber leaves powder	15	4–5	Wan Ngah and Hanafiah [21]
Sour orange residue	21.7	4–6	Khormaei et al. [22]
Wheat shell	10.8	5	Basci et al. [20]
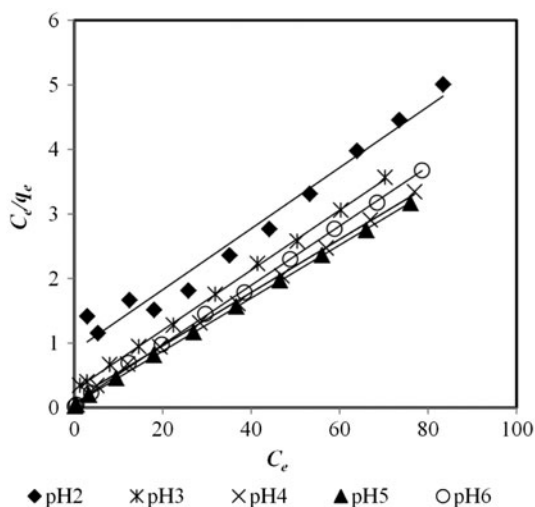
Fig. 5. Langmuir isotherm at different pH at constant temperature of 30℃.
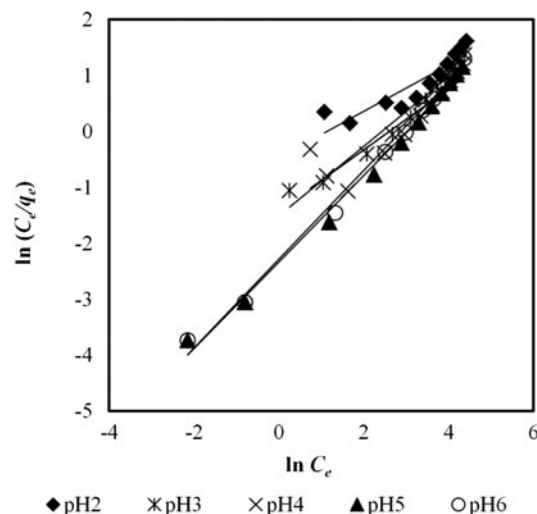
Fig. 7. R–P isotherm for different pH at constant temperature of 30℃.
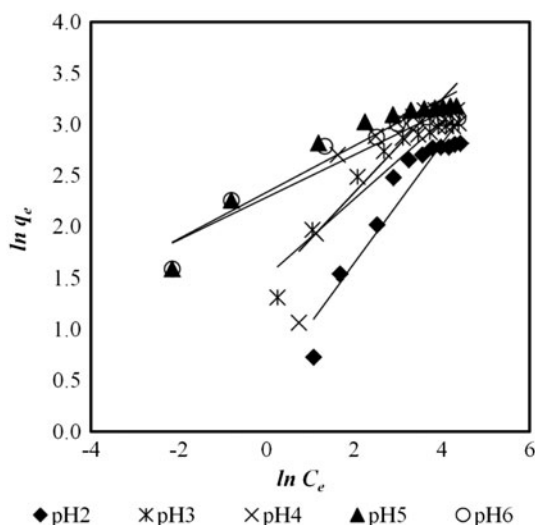
Fig. 6. Freundlich isotherm for different pH at constant temperature of 30℃.

equation shown in Table 1. The linearised form of Freundlich isotherm is plotted as $\ln q_e$ versus $\ln C_e$ and is shown in Fig. 6. The values of K_F and n were found and are given in Table 4. All the values of intensity of adsorption (n) are greater than one indicating a favourable physiosorption; where n represents the bond energies between Cu(II) ion and adsorbent [68]. The relative adsorption capacity K_F increases with an increase in pH.

R–P isotherm is a three-parameter model incorporating the features of the Langmuir and the Freundlich isotherms into a single equation shown in Table 1 and plotted in Fig. 7. The R–P adsorption

model dissolves to Langmuir form for $\beta = 0$ and second Henry's law for $\beta = 1$. The values of the R–P isotherm parameters a_R, $K_{R–P}$, β and the correlation coefficient R^2 for adsorption of Cu(II) onto the adsorbents SLP are presented in Table 4. The values of β for all the adsorbents lie between 0 and 1, indicating favourable adsorption. The values of $K_{R–P}$ indicate that the adsorption capacity of SLP increased with increasing pH. The higher correlation coefficient values also signify well, the prediction of the experimental data by the R–P model.

For different pH, the Temkin isotherms are plotted in Fig. 8 and isotherm parameters computed for Cu(II) adsorption onto the SLP are listed in Table 4. It is observed that the values of the correlation coefficients (R^2) are in the range of 0.96–0.98, signifying satisfactory representation of the equilibrium experimental data with the Temkin equation (Table 1) for sorption model. It can therefore be presumed that the Cu(II) adsorption is characterised by uniform distribution of binding energy and the heat of adsorption of the molecules in the layer decreases linearly with coverage of the adsorbate on the surface of the adsorbent particles [69].

D–R isotherm is another isotherm equation proposed by Dubinin having characteristics of the sorption curves, which are related to the porosity of the adsorbent [70]. The linear form of the D–R isotherm is given in Table 1 and plotted in Fig. 9. Where $K_{D–R}$ is related to the adsorption energy and q_{max} is the maximum adsorption capacity, ε is the Polanyi potential and E is the mean energy of sorption. The D–R isotherm parameters for the adsorption of Cu(II) are estimated and shown in Table 4. It is observed
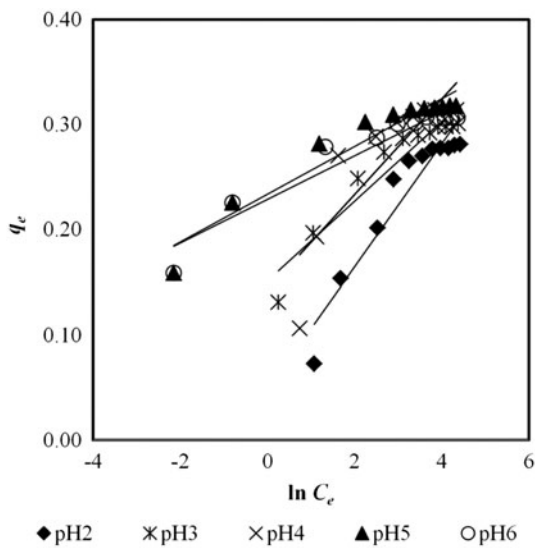
Fig. 8. Temkin isotherm for different pH at constant temperature of 30℃.
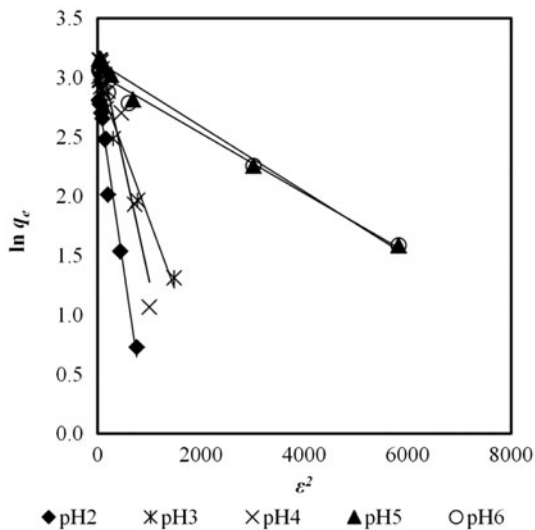
Fig. 9. D–R isotherm for different pH at constant temperature of 30℃.

that the theoretical maximum adsorption capacity as evaluated using D–R equation is the highest for the adsorbents at pH 4. The mean free energy of adsorption, E, estimated using the Polanyi Potential and the D–R isotherm constants were in the range of 0.43–1.33 kJ mol^{-1}, which signifies of physical adsorption reaction due to weak van der Waals forces. It is known that if the magnitude of the mean free energy lies between 8 and 16 kJ mol^{-1}, the mechanism of adsorption process can be explained by chemisorption or ion exchange [71,72]. It has also been observed that the values of the correlation coefficients for the D–R

isotherm plots are the lowest in comparison to the other four different isotherm models used for this study. It can therefore be concluded that the D–R equation does not represent the experimental data satisfactorily.

The adsorption studies and modelling of the data into various isotherms showed that the Cu(II) adsorption onto SLP follows the Langmuir isotherm, D–R isotherm at all pH levels as well as R–P isotherm at pH 3, 5 and 6. Thus, it can be concluded that adsorption is monolayer. Several researchers have also investigated the effect of pH on biosorption of Cu(II) by using different bioadsorbents and found similar results (Table 5). Langmuir model presented the best adjustment for Cu(II) removal by SLP with high regression coefficient.

3.3.3. Effect of temperature

The effect of temperature on the adsorption of Cu(II) onto the SLP is plotted in the form of Langmuir (Fig. 10), Freundlich (Fig. 11), R–P (Fig. 12), Temkin (Fig. 13) and D–R (Fig. 14) isotherms. The estimated isotherm parameters are represented in Table 6.

The adsorption of Cu(II) onto SLP at different temperatures is well correlated by Langmuir isotherm model in comparison with Freundlich and Temkin isotherms which give lower correlation coefficients. The adsorption equilibrium data were well fitted in the Langmuir isotherm, which signifies that the surface is uniform and all adsorption active sites are equivalent. For favourable adsorption, Freundlich constant (n) tends to have values between 0.1 and 1. Smaller value of n implies stronger interaction
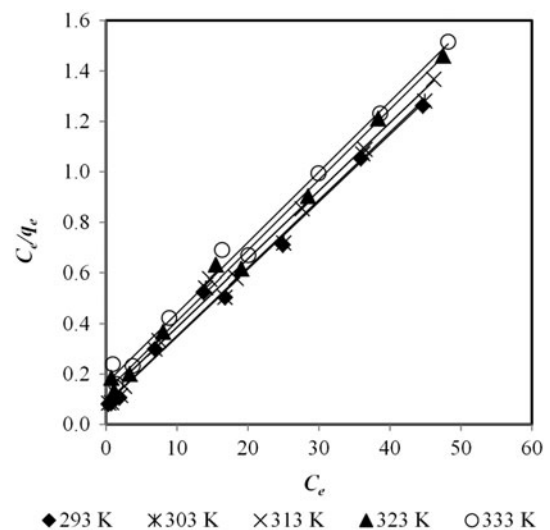
Fig. 10. Langmuir isotherm for different temperatures at constant pH of 5.
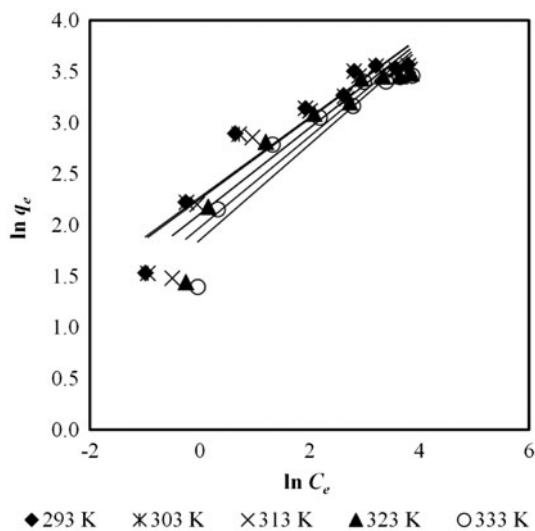
Fig. 11. Freundlich isotherm for different temperatures at constant pH of 5.
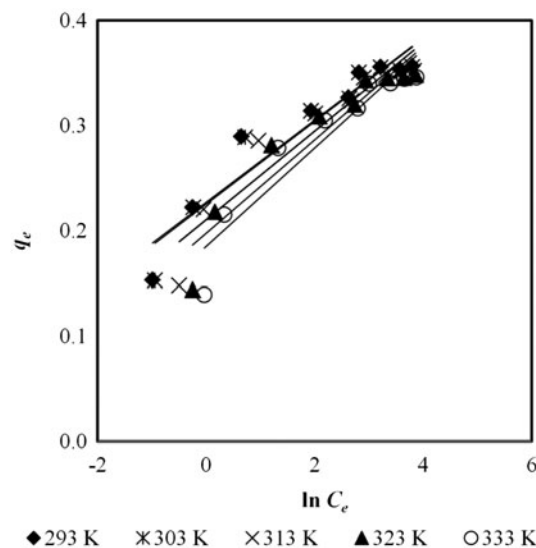
Fig. 13. Temkin isotherm for different temperatures at constant pH of 5.
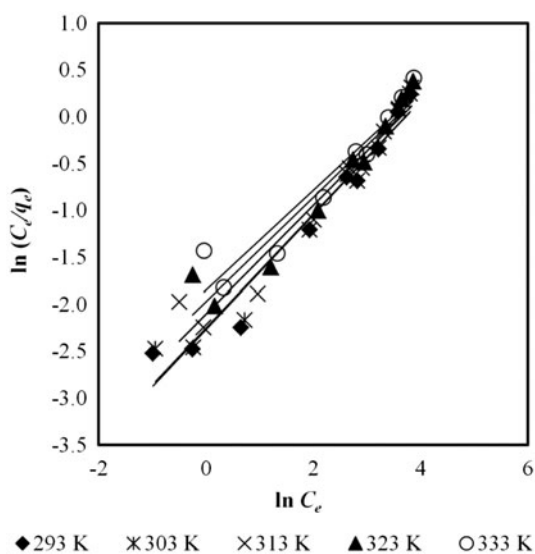
Fig. 12. R–P isotherm for different temperatures at constant pH of 5.
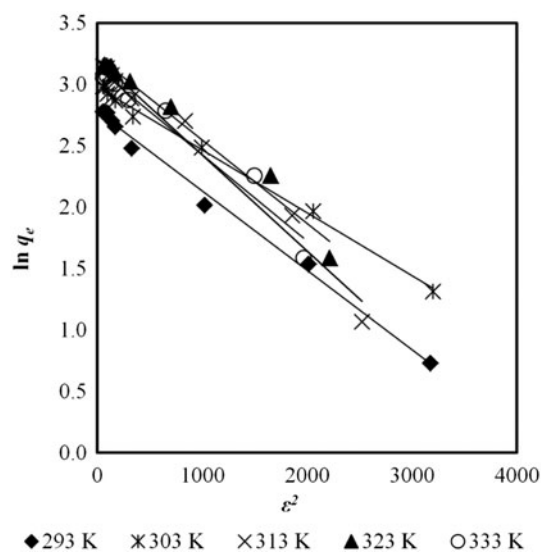
Fig. 14. D–R isotherm for different temperatures at constant pH of 5.

between solute and adsorbent, while n equal to 1 indicates linear adsorption leading to identical adsorption energies for all sites. A value for $n < 1$ indicates a normal Langmuir isotherm while $n > 1$ is indicative of cooperative adsorption [73]. Therefore, the adsorbed Cu(II) do not interact or compete with each other. Moreover, the monolayer is formed at the adsorbent surface and equilibrium is established.

From Table 6, the maximum adsorption capacity (q_{max}) calculated from Langmuir isotherm equation defines the total capacity of the adsorbent. The adsorption capacity decreased from 37.45 to 35.81 mg/g with an increasing of temperature from 293 to 333 K. The q_{max} values decreased with the increasing of temperature reveals that the adsorption process was favourable at low temperature and exothermic in nature, while the opposite trend indicates the process absorbs energy (endothermic). Several studies have been conducted using various types of adsorbents for Cu(II) adsorption. Again, to confirm the favourability of the adsorption process, the seperation factor is calculated and presented in Table 6. The values were found to lie between 0 and 1, confirming that the ongoing adsorption process is favourable.

Table 6
Constants and regression for different adsorption isotherms at different temperatures

Isotherm	Parameters	293 K	303 K	313 K	323 K	333 K
Langmuir	q_{max} (mg/g)	37.45	37.17	36.76	35.84	35.81
	K_L (L/mg)	0.0045	0.0036	0.0030	0.0022	0.0018
	R_L	0.306	0.354	0.403	0.478	0.526
	R^2	0.99	0.99	1.00	0.99	0.99
Freundlich	n	0.40	0.39	0.42	0.44	0.47
	K_F (L/g)	9.67	9.51	8.20	7.19	6.36
	R^2	0.91	0.91	0.90	0.90	0.90
Redlich–Peterson	β	2.27	2.25	2.10	1.97	1.85
	K_{R-P} (L/g)	0.61	0.61	0.58	0.56	0.53
	R^2	0.96	0.96	0.94	0.93	0.92
Temkin	A (L/mg)	2.62	2.62	2.57	2.54	2.50
	$K = RT/b$	6.58	6.59	6.83	6.94	7.10
	R^2	0.97	0.97	0.98	0.98	0.98
Dubinin–Radushkevich	q_{max} (mg/g)	33.85	33.65	30.39	32.40	31.89
	B	0.0006	0.0006	0.0011	0.0009	0.0010
	E (kJ/mol)	0.94	0.94	0.70	0.77	0.73
	R^2	0.98	0.98	0.94	0.98	0.98

The mean energy of adsorption values were in the range of physical adsorption reactions. Although the correlation coefficients of D–R plots are lower than that of Langmuir plots, q_{max} values are consistent with the experimental values. On the other hand, q_{max} values slightly decrease with temperature increase, confirming the exothermic process [74]. In light of the above discussion, the D–R isotherm is more applicable.

3.3.4. Adsorption thermodynamics

The spontaneity of a process is determined by the values of thermodynamic parameters such as enthalpy change ($\Delta H°$), entropy change ($\Delta S°$) and Gibbs free energy change ($\Delta G°$). Standard Gibbs free energy is calculated by the following Eq. (7):

$$\Delta G° = -RT \ln K_L \tag{7}$$

where K_L (L/mol) is the equilibrium constant obtained from Langmuir model, T (K) is the absolute temperature and R (8.314 J/mol K) is the gas universal constant. The relationship between Gibbs free energy change, entropy change and enthalpy change can be expressed as shown below in Eq. (8):

$$\Delta G° = \Delta H° - T\Delta S° \tag{8}$$

Fig. 15 shows the plot of Gibbs free energy change versus temperature and the thermodynamic parameters $\Delta S°$ and $\Delta H°$ were calculated from the slope and intercept of the plot and are summarised in Table 7.

The Gibbs free energy is the measure of the degree of spontaneity and feasibility for the adsorption process. Higher the negative values of $\Delta G°$, more is the energetically favourable adsorption process [51]. Table 7 shows the decrease in the negative values of $\Delta G°$ with increasing temperature which indicated that the adsorption process of Cu(II) onto SLP was spontaneous in nature and the adsorption process was
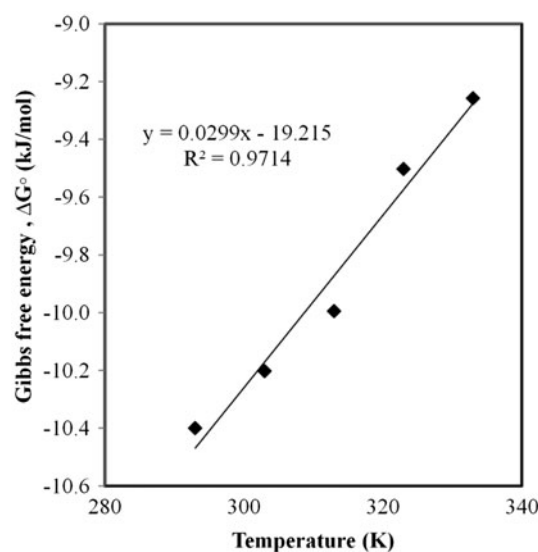
Fig. 15. Gibbs free energy change ($\Delta G°$) vs. the adsorption temperature.

Table 7
Thermodynamic parameters for adsorption of Cu(II) onto SLP in the aqueous solution

T (K)	K_L (L/mol)	$\Delta G°$ (kJ/mol)	$\Delta H°$ (kJ/mol)	$\Delta S°$ (kJ/mol K)
293	71.48	−10.40		
303	57.40	−10.20		
313	46.57	−10.00	−19.22	−0.23
323	34.42	−9.50		
333	28.33	−9.26		

more favourable at lower temperature. The negative value of $\Delta H°$ (−19.22 kJ/mol) implies that exothermic process occurred during adsorption of Cu(II). Moreover, it also predicts the adsorption as a physical adsorption. Negative value of $\Delta S°$ (−0.023 kJ/mol) denoted the decrease in randomness at the solid–solution interface during adsorption, resulting in the reversibility of the process [14]. Negative value of $\Delta S°$ suggested that decrease in randomness at the solid–solution interface during biosorption due to some structural alterations in the SLP biosorbent during metal binding [75].

3.4. Batch desorption studies

Desorption experiments were carried out in order to estimate the metal releasing capacity of SLP loaded with Cu(II) ions. As per the graphical results, HCl can be the most effective eluent for Cu(II) ions as it gave 90.9% desorption within 5 min; where 0.1 N HNO$_3$ and 0.1 N H$_2$SO$_4$ also gave 88.8 and 75% desorption, respectively, and attended the equilibrium after 8 min. Thus, HCl can be effectively used for the Cu(II) desorption. Adsorption capacity of biosorbent when checked repeatedly for five cycles of adsorption and desorption showed a decrease in the capacity by 18.7, 25.8, 36.9, 48.4% after each adsorption–desorption cycle. Remarkable decrease in the adsorption capacity of biosorbent after the fifth cycle makes it unfit for further use. However, no physical damage was observed to SLP biosorbent. Hence, further adsorption–desorption cycles were not studied. Thus, desorption process with 0.1 N HCl can be sufficiently applied to the real desorption system which can also be an economical and time-efficient process.

4. Conclusions

This study can be considered as a positive base for further study such as continuous process for heavy metal ions removal in model waste water and batch study using industrial wastewater, due to its effi-

ciency of Cu(II) adsorption in aqueous solution. The FT-IR spectrum showed the degradation of hydroxyl and carboxyl group as it formed complex with Cu(II). The SLP had significant adsorption capacity for Cu(II) ions about 29.32 mg/g. Adsorption is monolayer and depends upon particle size, pH and temperature. Cu(II) adsorption is maximum at pH 5 at lower temperature, i.e. 20°C. Desorption of Cu(II) ions can also be possible easily in acidic environment, specially 0.1 N HCl which has 90% elution property. The kinetic data was analysed using two kinetic models, particularly pseudo-first-order and pseudo-second-order. The pseudo-second-order kinetic model was found to agree well with the experimental data. The adsorption process was found to be controlled by three steps of diffusion mechanisms. The temperature and pH equilibrium data fitted well with Langmuir isotherm model and the monolayer adsorption capacity was found to be 37.45 mg/g at 293 K. Thermodynamic constants were also evaluated using equilibrium constants from Langmuir isotherm. The negative values of Gibbs free energy change ($\Delta G°$), enthalpy change ($\Delta H°$) and entropy change ($\Delta S°$) show that the process of adsorption of Cu(II) onto SLP is spontaneous, exothermic and favourable.

Abbreviations

q_e	—	equilibrium adsorption capacity (mg/g)
q_t	—	metal sorption capacity of the adsorbent at time t (mg/g)
k_1	—	the pseudo-first-order rate constant (min^{-1})
t	—	the contact time (min)
k_2	—	pseudo-second-order rate constant (g. mg^{-1} min^{-1})
C_0	—	initial concentration of Cu(II) ions in solution (mg/L)
C_e	—	equilibrium concentration of Cu(II) ions in solution (mg/L)
C_t	—	concentration of Cu(II) ions in solution at any time t (mg/L)
V	—	volume of liquid (L)
M	—	weight of the adsorbent (g)
q_{max}	—	maximum monolayer biosorption of the Cu(II) (mg/g)
K_L	—	Langmuir constant related to the affinity of binding sites (L mg^{-1})
K_F	—	Freundlich constant, it gives adsorption capacity of biosorbent (mg/g)
n	—	Freundlich exponent related to adsorption intensity (1/n is heterogeneity factor)
K_{R-P}	—	Redlich–Peterson isotherm constant (L g^{-1})

a_R	—	Redlich–Peterson constant ($L\,mg^{-1}$)
β	—	Redlich–Peterson exponent which lies between 1 and 0
A, b	—	Temkin constant related to heat of sorption (J/mol)
K_T	—	Temkin isotherm equilibrium binding constant ($L\,g^{-1}$)
R	—	universal gas constant ($8.314\,J\,K^{-1}\,mol^{-1}$)
T	—	the temperature (K)
B	—	gives the mean free energy E ($kJ\,mol^{-1}$) of sorption per molecule of the sorbate when it is transferred to the surface of the solid from infinity in the solution ($mol^2\,kJ^{-2}$)
E	—	the apparent energy of adsorption from Dubinin–Radushkevich isotherm model ($kJ\,mol^{-1}$)
$\Delta H°$	—	enthalpy change (kJ/mol)
$\Delta S°$	—	entropy change ($kJ/mol\,K$)
$\Delta G°$	—	Gibbs free energy change (kJ/mol)

References

[1] J.C. Igwe, A.A. Abia, A bioseparation process for removing heavy metals from waste water using biosorbents, Afr. J. Biotechnol. 5 (2006) 1167–1179.

[2] J.G. Dean, F.L. Bosqui, K.H. Lanouette, Removing heavy metals from waste water, Environ. Sci. Technol. 6 (1972) 518–522.

[3] J. Bouzid, Z. Elouear, M. Ksibi, M. Feki, A. Montiel, A study on removal characteristics of copper from aqueous solution by sewage sludge and pomace ashes, J. Hazard. Mater. 152 (2008) 838–845.

[4] T.A. Davis, B. Volesky, R.H.S. Vieira, *Sargassum* seaweed as biosorbent for heavy metals, Water Res. 34 (2000) 4270–4278.

[5] M. Liu, Y. Deng, H. Zhan, X. Zhang, Adsorption and desorption of copper(II) from solutions on new spherical cellulose adsorbent, J. Appl. Polym. Sci. 84 (2002) 478–485.

[6] E. Eren, Removal of copper ions by modified Unye clay, Turkey, J. Hazard. Mater. 159 (2008) 235–244.

[7] A.A. Augustine, B.D. Orike, A. Edidiong, Adsorption kinetics and modeling of Cu(II) ion sorption from aqueous solution by mercaptoacetic acid modified cassava (*Manihot sculenta cranz*) wastes, Electron. J. Environ. Agric. Food Chem. 6 (2007) 2221–2234.

[8] B. Kizilkaya, A.A. Tekinay, Y. Dilgin, Adsorption and removal of Cu(II) ions from aqueous solution using pretreated fish bones, Desalination 264 (2010) 37–47.

[9] Y. Nuhoglu, E. Malkoc, A. Gürses, N. Canpolat, The removal of Cu(II) from aqueous solutions by *Ulothrix zonata*, Biores. Technol. 85 (2002) 331–333.

[10] G. Patil, I. Ahmad, Heavy metals contamination assesment of Kanhargaon dam water near Chhindwara city, Acta Chim. Pharm. Indica 1 (2011) 7–9.

[11] M. Mukhopadhyay, S.B. Noronha, G.K. Suraishkumar, A review on experimental studies of biosorption of heavy metals by *Aspergillus niger*, Can. J. Chem. Eng. 89 (2011) 889–900.

[12] H. Xu, Y. Chen, H. Huang, Y. Liu, Z. Yang, Removal of lead (II) and cadmium (II) from aqueous solutions using spent *Agaricus bisporus*, Can. J. Chem. Eng. 91 (2013) 421–431.

[13] X. Li, Y. Tang, X. Cao, D. Lu, F. Luo, W. Shao, Preparation and evaluation of orange peel cellulose adsorbents for effective removal of cadmium, zinc, cobalt and nickel, Colloid Surf. A 317 (2008) 512–521.

[14] K.S. Tong, M.J. Kassim, A. Azraa, Adsorption of copper ion from its aqueous solution by a novel biosorbent *Uncaria gambir*: Equilibrium, kinetics, and thermodynamic studies, Chem. Eng. J. 170 (2011) 145–153.

[15] A. El-Sikaily, A. El Nemr, A. Khaled, O. Abdelwehab, Removal of toxic chromium from wastewater using green alga *Ulva lactuca* and its activated carbon, J. Hazard. Mater. 148 (2007) 216–228.

[16] S.E. Bailey, T.J. Olin, R.M. Bricka, D.D. Adrian, A review of potentially low-cost sorbents for heavy metals, Water Res. 33 (1999) 2469–2479.

[17] S.-H. Lee, J.-W. Yang, Removal of copper in aqueous solution by apple wastes, Sep. Sci. Technol. 32 (1997) 1371–1387.

[18] G. Annadurai, R.S. Juang, D.J. Lee, Adsorption of heavy metals from water using banana and orange peels, Water Sci. Technol. 47 (2003) 185–190.

[19] B. Nasernejad, T.E. Zadeh, B.B. Pour, M.E. Bygi, A. Zamani, Camparison for biosorption modeling of heavy metals (Cr(III), Cu(II), Zn(II)) adsorption from wastewater by carrot residues, Process Biochem. 40 (2005) 1319–1322.

[20] N. Basci, E. Kocadagistan, B. Kocadagistan, Biosorption of copper (II) from aqueous solutions by wheat shell, Desalination 164 (2004) 135–140.

[21] W.S. Wan Ngah, M.A.K.M. Hanafiah, Adsorption of copper on rubber (*Hevea brasiliensis*) leaf powder: Kinetic, equilibrium and thermodynamic studies, Biochem. Eng. J. 39 (2008) 521–530.

[22] M. Khormaei, B. Nasernejad, M. Edrisi, T. Eslamzadeh, Copper biosorption from aqueous solutions by sour orange residue, J. Hazard. Mater. 149 (2007) 269–274.

[23] G.A. Moore, Oranges and lemons: Clues to the taxonomy of Citrus from molecular markers, Trends Genet. 17 (2001) 536–540.

[24] D. Mamma, E. Kourtoglou, P. Christakopoulos, Fungal multienzyme production on industrial by-products of the citrus-processing industry, Biores. Technol. 99 (2008) 2373–2383.

[25] M.R. Ibrahim, H.M. El-Banna, I.I. Omara, M.A. Suliman, Evaluation of nutritive value of some Citrus pulp as feedstuffs in rabbit diets, Pak. J. Nutr. 10 (2011) 667–674.

[26] N. Vasudeva, T. Sharma, Chemical composition and antimicrobial activity of essential oil of Citrus limettioides tanaka, J. Pharm. Technol. Drug Res. 2 (2012) 1–7.

[27] F. Anwar, R. Naseer, M.I. Bhanger, S. Ashraf, F. Talpur, F. Aladedunye, Physico-chemical characteristics of Citrus seeds and seed oils from Pakistan, J. Am. Oil Cem. Soc. 85 (2008) 321–330.

[28] M. Senevirathne, Y.-J. Jeon, J.-H. Ha, S.-H. Kim, Effective drying of citrus by-product by high speed drying: A novel drying technique and their antioxidant activity, J. Food Eng. 92 (2009) 157–163.

[29] S.S. Dhillon, R.K. Gill, S.S. Gill, M. Singh, Studies on the utilization of citrus peel for pectinase production using fungus *Aspergillus niger*, Int. J. Environ. Stud. 61 (2004) 199–210.

[30] K.A. Krishnan, T.S. Anirudhan, Removal of cadmium(II) from aqueous solutions by steam-activated sulphurised carbon prepared from sugar-cane bagasse pith: Kinetics and equilibrium studies, Water S.A. 29 (2003) 147–156.

[31] E. Demirbas, N. Dizge, M.T.T. Sulak, M. Kobya, Adsorption kinetics and equilibrium of copper from aqueous solutions using hazelnut shell activated carbon, Chem. Eng. J. 148 (2009) 480–487.

[32] M.A. Acheampong, J.P.C. Pereira, R.J.W. Meulepas, P.N.L. Lens, Kinetics modelling of Cu(II) biosorption on to coconut shell and *Moringa oleifera* seeds from tropical regions, Environ. Technol. 33 (2012) 409–417.

[33] A. Ismail, D.B. Adie, I.A. Oke, J.A. Otun, N.O. Olarinoye, S. Lukman, C.A. Okuofu, Adsorption kinetics of cadmium ions onto powdered corn cobs, Can. J. Chem. Eng. 87 (2009) 896–909.

[34] A.R. Iftikhar, H.N. Bhatti, M.A. Hanif, R. Nadeem, Kinetic and thermodynamic aspects of Cu(II) and Cr(III) removal from aqueous solutions using rose waste biomass, J. Hazard. Mater. 161 (2009) 941–947.

[35] H. Benaïssa, M.A. Elouchdi, Removal of copper ions from aqueous solutions by dried sunflower leaves, Chem. Eng. Process. 46 (2007) 614–622.

[36] C.-S. Zhu, L.-P. Wang, W. Chen, Removal of Cu(II) from aqueous solution by agricultural by-product: Peanut hull, J. Hazard. Mater. 168 (2009) 739–746.

[37] G. Müller, K. Janošková, T. Bakalár, J. Cakl, H. Jiránková, Removal of Zn(II) from aqueous solutions using Lewatit S1468, Desalin. Water Treat. 37 (2012) 146–151.

[38] Y.S. Ho, G. McKay, Pseudo-second order model for sorption processes, Process Biochem. 34 (1999) 451–465.

[39] M.I. Panayotova, Kinetics and thermodynamics of copper ions removal from wastewater by use of zeolite, Waste Manage. (Oxford) 21 (2001) 671–676.

[40] O. Keskinkan, M.Z.L. Goksu, A. Yuceer, M. Basibuyuk, C.F. Forster, Heavy metal adsorption characteristics of a submerged aquatic plant (*Myriophyllum spicatum*), Process Biochem. 39 (2003) 179–183.

[41] A. Krobba, D. Nibou, S. Amokrane, H. Mekatel, A. Krobba, D. Nibou, S. Amokrane, H. Mekatel, Adsorption of copper (II) onto molecular sieves NaY, Desalin. Water Treat. 37 (2012) 37–37.

[42] M. Özacar, İ.A. Şengil, Adsorption of metal complex dyes from aqueous solutions by pine sawdust, Biores. Technol. 96 (2005) 791–795.

[43] I. Langmuir, The constitution and fundamental properties of solids and liquids. II. Liquids.1, J. Am. Chem. Soc. 39 (1917) 1848–1906.

[44] O. Redlich, D.L. Peterson, A useful adsorption isotherm, J. Phys. Chem. 63 (1959) 1024.

[45] Y. Liu, Y.-J. Liu, Biosorption isotherms, kinetics and thermodynamics, Sep. Purif. Technol. 61 (2008) 229–242.

[46] K.R. Ramakrishna, T. Viraraghavan, Dye removal using low cost adsorbents, Water Sci. Technol. 36 (1997) 189–196.

[47] K.V. Kumar, K. Porkodi, Relation between some two- and three-parameter isotherm models for the sorption of methylene blue onto lemon peel, J. Hazard. Mater. 138 (2006) 633–635.

[48] K. Vasanth Kumar, S. Sivanesan, Equilibrium data, isotherm parameters and process design for partial and complete isotherm of methylene blue onto activated carbon, J. Hazard. Mater. 134 (2006) 237–244.

[49] M.N.V. Prasad, H. Freitas, Removal of toxic metals from solution by leaf, stem and root phytomass of *Quercus ilex L.* (holly oak), Environ. Pollut. 110 (2000) 277–289.

[50] H. Aydın, Y. Bulut, Ç. Yerlikaya, Removal of copper (II) from aqueous solution by adsorption onto low-cost adsorbents, J. Environ. Manage. 87 (2008) 37–45.

[51] A.N. Kosasih, J. Febrianto, J. Sunarso, Y.-H. Ju, N. Indraswati, S. Ismadji, Sequestering of Cu(II) from aqueous solution using cassava peel (*Manihot esculenta*), J. Hazard. Mater. 180 (2010) 366–374.

[52] U. Suryavanshi, S.R. Shukla, Adsorption of Pb^{2+} by alkali-treated *Citrus limetta* peels, Ind. Eng. Chem. Res. 49 (2010) 11682–11688.

[53] Y.S. Ho, G. McKay, The sorption of lead(II) ions on peat, Water Res. 33 (1999) 578–584.

[54] H.D. Ozsoy, H. Kumbur, Adsorption of Cu(II) ions on cotton boll, J. Hazard. Mater. 136 (2006) 911–916.

[55] W. Plazinski, W. Rudzinski, A. Plazinska, Theoretical models of sorption kinetics including a surface reaction mechanism: A review, Adv. Colloid Interface 152 (2009) 2–13.

[56] S. Karthikeyan, R. Balasubramanian, C.S.P. Iyer, Evaluation of the marine algae *Ulva fasciata* and *Sargassum sp.* for the biosorption of Cu(II) from aqueous solutions, Biores. Technol. 98 (2007) 452–455.

[57] Z. Aksu, Y. Sag, T. Kutsal, The biosorpnon of copperod by *C. vulgaris* and *Z. ramigera*, Environ. Technol. 13 (1992) 579–586.

[58] A. Özcan, A.S. Özcan, S. Tunali, T. Akar, I. Kiran, Determination of the equilibrium, kinetic and thermodynamic parameters of adsorption of copper(II) ions onto seeds of *Capsicum annuum*, J. Hazard. Mater. 124 (2005) 200–208.

[59] G. Bayramoğlu, M.Y. Arıca, Ethylenediamine grafted poly(glycidylmethacrylate-co-methylmethacrylate) adsorbent for removal of chromate anions, Sep. Purif. Technol. 45 (2005) 192–199.

[60] X. Sun, X. Huang, X. Liao, B. Shi, Adsorptive removal of Cu(II) from aqueous solutions using collagen-tannin resin, J. Hazard. Mater. 186 (2011) 1058–1063.

[61] A.A. Özer, D. Özer, The adsorption of copper(II) ions on to dehydrated wheat bran (DWB): Determination of the equilibrium and thermodynamic parameters, Process Biochem. 39 (2004) 2183–2191.

[62] D. Özçimen, A. Ersoy-Meriçboyu, Removal of copper from aqueous solutions by adsorption onto chestnut shell and grapeseed activated carbons, J. Hazard. Mater. 168 (2009) 1118–1125.

[63] S. Liang, X. Guo, N. Feng, Q. Tian, Effective removal of heavy metals from aqueous solutions by orange peel xanthate, Trans. Nonferrous Met. Soc. Chin. 20 (2010) s187–s191.

[64] A.E. Ofomaja, E.B. Naidoo, S.J. Modise, Dynamic studies and pseudo-second order modeling of copper(II) biosorption onto pine cone powder, Desalination 251 (2010) 112–122.

[65] C.-H. Weng, Y.-C. Wu, Potential low-cost biosorbent for copper removal: Pineapple leaf powder, J. Environ. Eng. 138 (2011) 286–292.

[66] M. Ajmal, A. Hussain Khan, S. Ahmad, A. Ahmad, Role of sawdust in the removal of copper(II) from industrial wastes, Water Res. 32 (1998) 3085–3091.

[67] P. SenthilKumar, S. Ramalingam, R.V. Abhinaya, S.D. Kirupha, T. Vidhyadevi, S. Sivanesan, Adsorption equilibrium, thermodynamics, kinetics, mechanism and process design of zinc(II) ions onto cashew nut shell, Can. J. Chem. Eng. 90 (2012) 973–982.

[68] G. McKay, Adsorption of dyestuffs from aqueous solutions with activated carbon I: Equilibrium and batch contact-time studies, J. Chem. Technol. Biotechnol. 32 (1982) 759–772.

[69] Y. Kim, C. Kim, I. Choi, S. Rengaraj, J. Yi, Arsenic removal using mesoporous alumina prepared via a templating method, Environ. Sci. Technol. 38 (2003) 924–931.

[70] M.M. Dubinin, The potential theory of adsorption of gases and vapors for adsorbents with energetically nonuniform surfaces, Chem. Rev. 60 (1960) 235–241.

[71] S. Maity, S. Chakravarty, S. Bhattacharjee, B.C. Roy, A study on arsenic adsorption on polymetallic sea nodule in aqueous medium, Water Res. 39 (2005) 2579–2590.

[72] P.B. Bhakat, A.K. Gupta, S. Ayoob, S. Kundu, Investigations on arsenic(V) removal by modified calcined bauxite, Colloid Surf. A 281 (2006) 237–245.

[73] B.H. Hameed, A.L. Ahmad, K.N.A. Latiff, Adsorption of basic dye (methylene blue) onto activated carbon prepared from rattan sawdust, Dyes Pigm. 75 (2007) 143–149.

[74] J.S. Piccin, G.L. Dotto, L.A.A. Pinto, Adsorption isotherms and thermochemical data of FD & C Red n° 40 binding by Chitosan, Braz. J. Chem. Eng. 28 (2011) 295–304.

[75] Z. Aksu, Determination of the equilibrium, kinetic and thermodynamic parameters of the batch biosorption of nickel(II) ions onto *Chlorella vulgaris*, Process Biochem. 38 (2002) 89–99.